Sustainable Energy & Fuels

ROYAL SOCIETY OF CHEMISTRY

PAPER

View Article Online
View Journal | View Issue

Cite this: *Sustainable Energy Fuels*, 2023, 7, 4254

Power factor improvement in a solid–liquid thermoelectric system formed by Sb:SnO_2 in contact with a chromium complex solution†

S. Castro-Ruiz,[a] L. Márquez-García,[a] M. Solis-de la Fuente,[a] B. Beltrán-Pitarch,[a] A. Mota-Babiloni,[a] F. Vidan,[a] P. Íñigo-Rabinal,[b] G. Guisado-Barrios[b] and J. García-Cañadas *[a]

Thermoelectric (TE) materials can convert heat into electricity. Good TE materials should have high power factors (PF) and low thermal conductivities. PF = $S^2\sigma$ is governed by the Seebeck coefficient S and the electrical conductivity σ. Most recent improvements in TE materials performance have been achieved by the reduction of the thermal conductivity, and strategies to improve the PF have been minor. Recently, an innovative concept to significantly increase the PF, based on the combination of a porous TE solid with an electrolyte, has been reported. Here, we make use of this new approach but using an electroactive salt (redox molecule) solution as electrolyte, rather than the non-electroactive electrolytes and ionic liquids previously employed. A system formed by a nanostructured and porous Sb:SnO_2 film in contact with Cr(III) acetylacetonate dissolved in 3-methoxypropionitrile was prepared. Using this electrolyte, an average PF enhancement of 3.4 times was achieved, due to an average decrease of 23.2% and 82.8% in the absolute value of the Seebeck coefficient and the electrical resistivity of the solid, respectively. An impedance spectroscopy analysis, after checking by scanning electron microscopy and energy-dispersive X-ray spectroscopy that no changes take place in the Sb:SnO_2 film due to the presence of electrolytes, revealed that the improvements come from the donation of electrons from the electrolyte to the solid, which increases its electrical conductivity and the usual drop in the Seebeck coefficient. The remarkable PF improvement obtained is among the highest reported and opens a new way of significantly enhancing this parameter.

Received 11th May 2023
Accepted 21st July 2023

DOI: 10.1039/d3se00622k

rsc.li/sustainable-energy

Introduction

More than 60% of the global power is lost as waste heat. In addition to the waste heat, ubiquitous heat sources such as the sun or even our own bodies are widely available. Thermoelectric (TE) devices can directly convert heat into electricity under safe, clean, and environmentally friendly operation.[1,2] Due to this, TEs can be used in radioisotope TE generators for spacecrafts, as solar TE generators, in automobiles and industries utilizing heat from hot exhausts as heat source, and to power wearable devices and sensors, among other applications.[3,4] A good TE material should have a high power factor (PF) and a low thermal conductivity. PF = $S^2\sigma$ is determined by the Seebeck coefficient S and the electrical conductivity σ. Some of the most significant recent improvements in TE materials performance have been mainly achieved by the reduction of the thermal conductivity, but strategies to improve the PF have been less successful,[5,6] since they require decoupling the Seebeck coefficient from the electrical conductivity.[7,8]

Recently, an innovative approach to increase the PF has shown above 3 times improvements of this parameter, which are among the highest reported.[9] This new concept is based on the combination of a nanostructured and porous TE solid that is permeated with an electrolyte, with the intention of improving the TE properties of the solid by means of different interactions that can occur with the electrolyte. In that study, using an Sb-doped SnO_2 film as a solid, and 1 M $LiBF_4$ dissolved in 3-methoxypropionitrile (3-MPN) as the electrolyte, the PF was increased 3.4 times. The enhancement was due to a more than 60% decrease in the electrical resistivity of the solid without a significant variation of the Seebeck coefficient. In addition, the ionic liquid 1-butyl-3-methylimidazolium iodide was also employed as electrolyte, and showed an enhancement of 2.4 times in the PF, due to a more than 82% decrease in the electrical resistivity and a 35% reduction in the absolute value of the Seebeck coefficient.

[a]*Department of Industrial Systems Engineering and Design, Universitat Jaume I, Av. Vicent Sos Baynat s/n, 12006 Castelló de la Plana, Spain. E-mail: garciaj@uji.es*
[b]*CSIC-Universidad de Zaragoza, Institute for Chemical Synthesis and Homogeneous Catalysis (ISQCH), C/Pedro Cerbuna 12, 50009 Zaragoza, Spain*

† Electronic supplementary information (ESI) available. See DOI: https://doi.org/10.1039/d3se00622k

Here, we explore the use of a different kind of electrolyte in this promising solid-electrolyte system. Unlike the previously employed non-electroactive salts, such as $LiBF_4$, and the ionic liquids, we have used a solution of an electroactive molecule as electrolyte. Electroactive species, also known as redox molecules, are able to exchange electrons with the nanostructured solid, which could lead to new mechanisms of PF improvements in the hybrid system. Inorganic complexes are common electroactive species. For our study, we have chosen a Cr(III) acetylacetonate [$Cr(acac)_3$] complex dissolved in the 3-MPN organic solvent. As TE solid we used the same Sb-doped SnO_2 film. In this different system, we show that significant PF improvements are also found. Moreover, using impedance spectroscopy, we analyze the mechanisms that lie behind these identified improvements.

Experimental section

Nanostructured and porous Sb:SnO_2 films were fabricated using microscope slide glasses of 25 mm × 15 mm size and 1 mm thickness as substrates. They were cleaned before film deposition by means of three sonication steps of 15 min in different media. In the first step, sonication was performed using a soap (Labkem, SOAP-0685K0)/water solution (1 : 10 v/v). Then, in the second step, distilled water was used to remove excess soap. Finally, isopropanol (Labkem, PROL-P0P-5K0) medium was employed for sonication. After this, substrates were dried under a compressed air flow and treated in a UV ozone cleaner (Ossila, L2002A2-UK) for 20 min. Subsequently, an Sb:SnO_2 colloidal aqueous dispersion (Keeling & Walker, A20W) was deposited by spin coating (Laurell, WS-650MZ-23NPPB) at 2500 rpm for 15 s, covering a centered area of the substrate of 10 mm × 5 mm. A total of four layers were deposited. After each deposition, a drying process was carried out on a hot plate at 100 °C for 10 min. Finally, the films were annealed at 550 °C for 45 min in a furnace (Nabertherm, 400-1) with a 3 °C min^{-1} heating rate. Scanning electron microscopy (SEM) images of the films and their composition were obtained using a JEOL 7001F instrument (Oxford Instruments) with energy-dispersive X-ray spectroscopy (EDX). The films' structure before and after annealing was tested by X-ray diffraction (XRD) using a Bruker D4-Endeavor instrument.

The films were contacted at their ends by Pt contacts, which were deposited by sputtering (Quorum, Q300T D Plus) for 60 s after growing an initial Cr seeding layer for 15 s (see Fig. 1a). A 0.1 M solution of chromium(III) acetylacetonate [$Cr(acac)_3$] (Sigma Aldrich, ref. 202031-5G) dissolved in the high boiling point organic solvent 3-methoxypropionitrile (3-MPN) (Sigma Aldrich, ref. 65290-250MK-F) was employed as electrolyte. All the compounds were used as received and handled in a glovebox (MBRAUN, Labstar 4516) under inert atmosphere conditions to avoid the presence of moisture. The stock electrolyte solution was prepared in a sealed vial with a septum, and stored under vacuum (pressure of −1 bar) before use. Nuclear magnetic resonance (NMR) spectra were recorded on Bruker spectrometers operating at 300 MHz (^{1}H NMR) and referenced to $SiMe_4$ (δ in ppm and J in Hertz). ^{1}H NMR experiments were recorded at room temperature in CD_3CN (Sigma Aldrich, ref. 151807-25G) for both the 3-MPN solvent and the 0.1 M [$Cr(acac)_3$] solution prepared.

The Seebeck coefficient and the electrical resistance were measured in a homemade setup (see Fig. 1b to d) inside a glovebox (Sicco, WV 1992-08-55) under a N_2 flow. In order to establish a temperature difference in the setup, two copper blocks were used. One of them, with 3 cartridge heaters inserted (Watlow, ref. C1E13-L12) and 30 mm × 30 mm × 10 mm dimensions, acted as the heat source. A second larger copper block (50 mm × 50 mm × 30 mm) was used as the heat sink

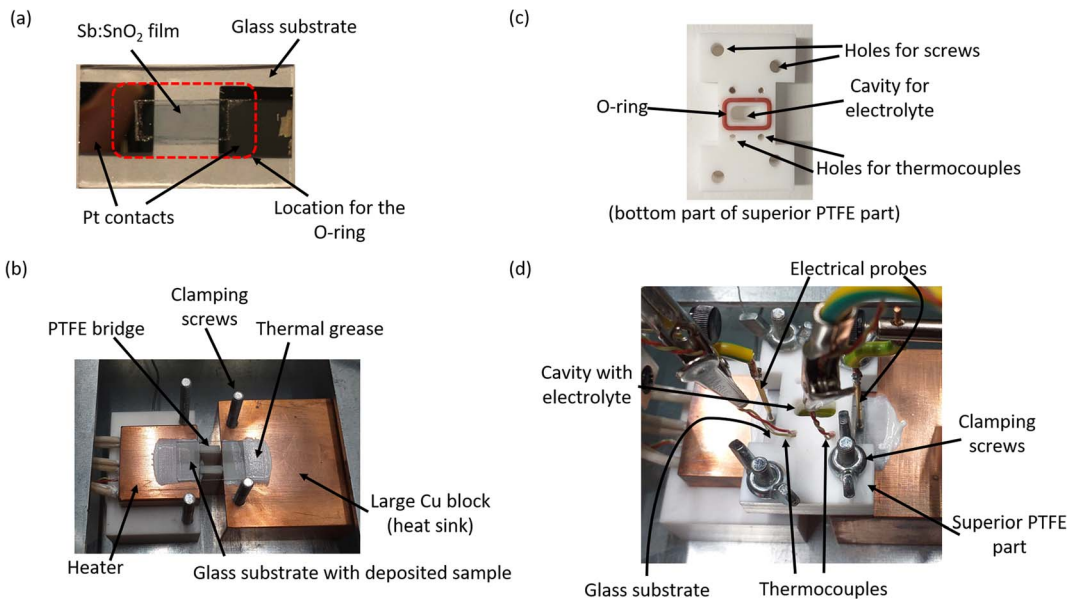

Fig. 1 Photographs of (a) the contacted film prepared, (b) the characterization setup with the top PTFE block not assembled, (c) the bottom part of the top PTFE block, and (d) the complete setup assembled.

(see Fig. 1b). The glass substrate with the film deposited was placed on top of the copper blocks, which are separated by a polytetrafluoroethylene (PTFE) bridge (see Fig. 1b). The latter helps to avoid breaking the sample during the time a pressure is applied by an O-ring. Thermal grease (RS, ref. 2173835) was used at the substrate/copper interfaces to improve the thermal contacts.

A holed PTFE block with a rectangular O-ring at the bottom side was placed on top of the glass substrate to allow the location of the electrolyte (see Fig. 1c). The location of the O-ring pressing the film can be seen in Fig. 1a. It should be noted that the pressure is held on the Pt contacts, not on the Sb-doped SnO_2 film. The PTFE block also has holes for positioning two thermocouples and several screws to provide a gentle pressure for sealing and avoiding liquid electrolyte leakage. Two K-type thermocouples (RS, ref. 8140134) were placed on top of the glass substrate aligned at the ends of the Pt contacts through the PTFE holes with a bit of thermal grease at their tips for thermalization (Fig. 1d). The electric contacts to the external circuit were made with two spring probes (RS, ref. 2615092) contacting at the edges of the Pt contacts, as shown in Fig. 1d.

Seebeck coefficient values were obtained from the slope of the open-circuit potential V_{oc} *versus* temperature difference ΔT plot. The V_{oc} was measured with a Keithley 2182A nanovoltmeter, and the temperature difference was varied in steps of $\approx$1 K from 0 up to $\approx$5 K by powering the cartridge heaters by means of a Watlow EZ-Zone PM temperature controller. The film electrical resistance R was obtained from the slope of the current–voltage I–V curve under no temperature difference. The I–V curves were measured using a Keithley 2450 source meter in 4-probe mode, scanning the current with a delay time of 2 s. Two spring probes contacted the Pt contacts at each side. In this way, the parasitic resistance of the cables could be removed, and only the electrical resistance of the film and the Pt/film contact is taken into account. Since the resistance of the film is expected in the order of kΩ (as will be shown below), the electrical contact resistance can be neglected. All the electrical measurements were recorded using coaxial cables, to avoid electrical interferences from the surroundings. The relative errors of the slopes from the fittings to the corresponding plots for S and R were lower than 2% and 1%, respectively, for both parameters.

Impedance spectroscopy measurements using the same 4-probe configuration as described above were performed under $\Delta T = 5$ K. Measurements were conducted in galvanostatic mode in the 1–0.01 Hz frequency range, using a dc current value of 0 A and 10 nA amplitude. A Metrohm-Autolab PGSTAT204 instrument, equipped with a FRA32M frequency response analyzer was employed for these measurements.

Results and discussion

Fig. 2 shows the SEM images of the different Sb:SnO_2 films prepared. Fig. 2a and b correspond to a film before being in contact with an electrolyte. It can be seen that the film is formed by interconnected nanoparticles of sizes from 6 to 10 nm. The presence of pores in the 2-50 nm range can also be observed. From Fig. 2b, the film thickness was estimated to be around 0.9 μm. Fig. 3 shows the XRD patterns of an Sb:SnO_2 film before and after the annealing. In both cases, a single phase was identified (cassiterite SnO_2, R040017, RRUFF Database), which is not modified after the annealing process. In addition, no additional peaks were found due to Sb, indicating that it acts as

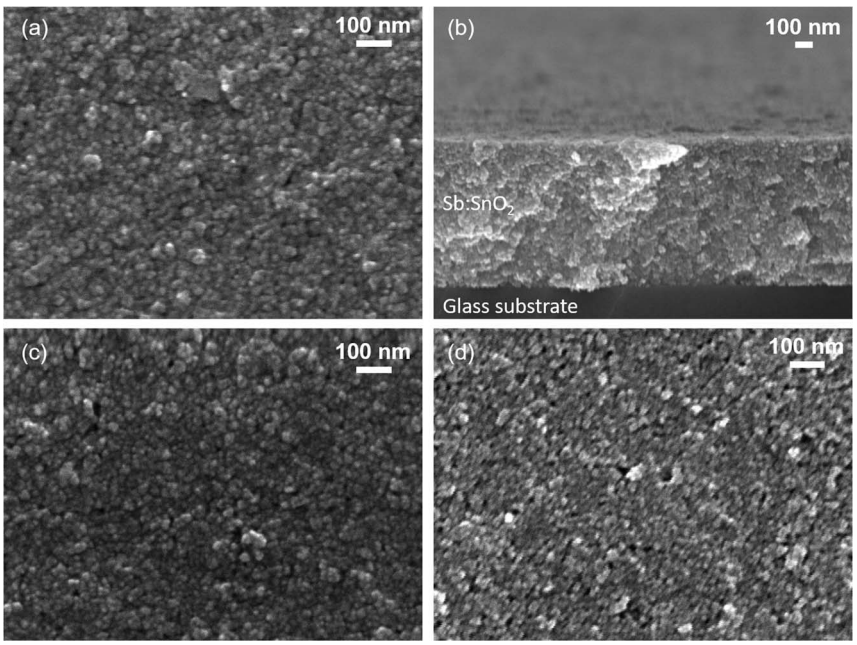

Fig. 2 (a) Top and (b) cross-section SEM images of an Sb-doped SnO_2 film before being in contact with an electrolyte. Top SEM images of an Sb:SnO_2 film after being in contact with (c) the 0.1 M $Cr(acac)_3$ solution in 3-MPN and (d) with only 3-MPN.

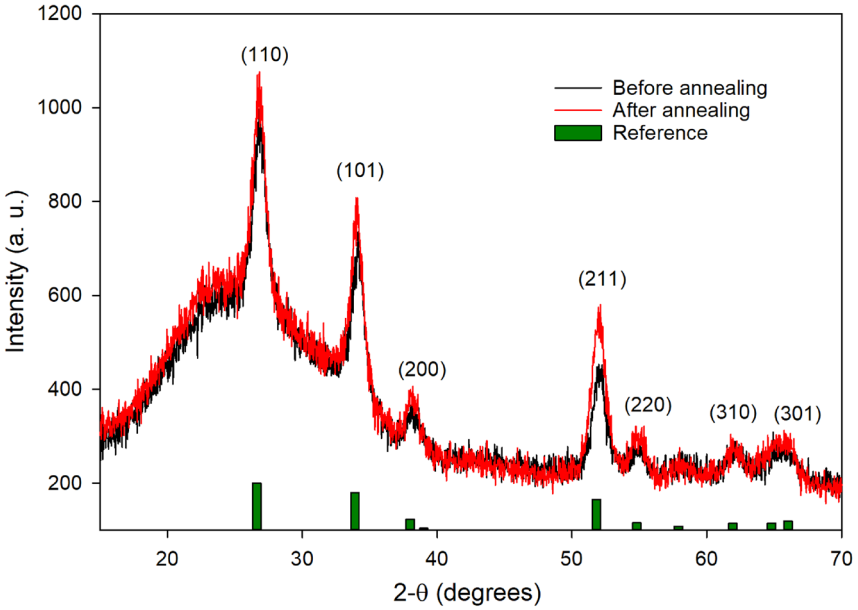

Fig. 3 XRD patterns of an Sb:SnO_2 film deposited on a glass substrate before and after annealing. The reference bars correspond to the indexation of the diffraction peaks for SnO_2 cassiterite (R040017, RRUFF Database).

a dopant in the structure. It should be noted that the broad background peak that appears at the lower 2θ values is due to the glass substrate, which lies underneath the film.

The TE properties of the different systems evaluated can be seen in Table 1. These properties are obtained from the measurements shown in Fig. S1 and S2.† First, three Sb:SnO_2 films without and with the $Cr(acac)_3$ electrolyte were tested (films 1-Cr to 3-Cr). Then, a configuration without the presence of the oxide film, just the Pt contacts and the $Cr(acac)_3$ electrolyte, was analyzed (No film). Finally, three Sb:SnO_2 films without and with only the 3-MPN solvent as electrolyte [without $Cr(acac)_3$] were measured (films 1-3MPN to 3-3MPN). Fig. S1† shows the V_{oc}–ΔT and I–V plots for the films 1-Cr to 3-Cr, with and without the presence of the $Cr(acac)_3$ electrolyte, and Fig. S2† shows the same plots for the films 1-3MPN to 3-3MPN.

Films 1-Cr to 3-Cr were measured first without the presence of the electrolyte. Then, they were tested after the $Cr(acac)_3$ electrolyte was injected and a steady state value of the V_{oc} was observed, which in some cases took several hours. As can be seen in Table 1, the absolute value of the Seebeck coefficient decreased by an average value of 23.2% due to the presence of the electrolyte. On the other hand, a significant average drop of 82.8% in the electrical resistance was found, therefore, an average 3.4 times improvement in the PF was obtained (see Table 1). This remarkable PF improvement is the same as the highest reported in our previous study,[9] which was obtained using a 0.1 M $LiBF_4$ solution in 3-MPN as electrolyte. In order to rule out that the reduction in the resistance could be due to electrical conduction through the electrolyte, a configuration with only the electrolyte and the Pt contacts (No film) was measured. A high electrical resistance of 890 kΩ was found, which indicates that the electronic transport is only taking place through the oxide film. Due to this large resistance value, the Seebeck coefficient could not be determined for the No film configuration, since the instrument could not properly measure the V_{oc}.

Table 1 Seebeck coefficient and resistance of the different systems evaluated, indicating the variations of these parameters and the power factor (PF) improvements produced. Temperatures at which the measurements were performed are also indicated in brackets. For the Seebeck coefficient measurements they correspond to the temperature when $\Delta T = 0$

	Seebeck coefficient (μV K^{-1})			Electrical resistance (kΩ)			
	Without electrolyte	With electrolyte	Variation (%)	Without electrolyte	With electrolyte	Variation (%)	$PF_{with}/PF_{without}$
1-Cr	−57.5 (18.4 °C)	−44.4 (21.0 °C)	−23.5	11.1 (20.2 °C)	1.87 (22.6 °C)	−83.2	3.49
2-Cr	−57.9 (18.8 °C)	−43.8 (21.6 °C)	−24.3	11.8 (20.7 °C)	1.95 (22.1 °C)	−83.5	3.48
3-Cr	−57.6 (19.3 °C)	−45.0 (20.1 °C)	−21.9	11.4 (20.4 °C)	2.07 (22.3 °C)	−81.8	3.34
No film	—	—	—	—	890 (17.9 °C)	—	—
1-3MPN	−53.4 (12.2 °C)	−40.4 (17.9 °C)	−24.2	7.44 (15.0 °C)	4.33 (19.9 °C)	−41.8	0.99
2-3MPN	−51.3 (14.2 °C)	−39.2 (19.8 °C)	−23.4	10.0 (17.1 °C)	6.25 (20.8 °C)	−37.6	0.94
3-3MPN	−52.1 (13.2 °C)	−39.3 (18.4 °C)	−24.5	8.20 (16.2 °C)	4.61 (20.4 °C)	−43.7	1.01

To investigate further the role of the $Cr(acac)_3$ complex, three identical systems consisting of $Sb:SO_2$ and only the 3-MPN solvent in the electrolyte [no $Cr(acac)_3$ complex] were tested (1-3MPN to 3-3MPN in Table 1). In this case, the absolute value of the Seebeck coefficient drops to an average value of 24.0%, similar to the case of the system with the Cr complex in the electrolyte. On the other hand, the resistance experiences an average drop of 41.0%, which is lower than the 82.8% drop achieved in the Cr complex system. The observed variations led to basically no average variation of the PF. This clearly indicates that the Cr complex is necessary in the electrolyte to produce the PF improvements and to achieve lower resistance values. It should be noted that the temperatures at which the different experiments from Table 1 were performed differ in many cases, since it is very difficult to control the ambient temperature of the laboratory. Although significant changes in temperature could produce variations of the properties determined, the variations observed between the systems without and with electrolyte are below 3 °C for the Cr complex electrolyte, and below 6 °C for only 3-MPN cases. These not very large temperature differences cannot produce the variations observed in the TE parameters (S and R). In order to verify this, we measured the variation with temperature of S and R for one of the films (without the presence of electrolyte). Results can be seen in Fig. S4,† which shows very small changes in both properties with temperature.

In order to investigate whether the variations of the TE properties observed in Table 1 come from possible changes in the morphology and composition of the films, both parameters were analyzed by SEM and EDX, respectively. Top view SEM images of films before coming into contact with electrolytes and after exposure to the 0.1 M solution of the $Cr(acac)_3$ complex and to only 3-MPN are shown in Fig. 2. It can be seen that all the films show a similar morphology; no significant differences are found. On the other hand, the chemical compositions of the films shown in the SEM images are presented in Table 2. It can be seen that no significant changes occur again. Thus, the variation of the TE properties identified in Table 1 is not due to changes produced in the morphology or chemical composition of the films.

Table 2 Chemical compositions obtained by EDX for three different $Sb:SnO_2$ films: (i) before coming into contact with an electrolyte, (ii) after coming into contact with a 0.1 M $Cr(acac)_3$ solution in 3-MPN and (iii) after exposure to only 3-MPN

Element	Film	Atomic%
Sn	Before contact with electrolyte	30.2
	After contact with the Cr complex solution	30.5
	After contact with only 3-MPN	30.4
Sb	Before contact with electrolyte	3.72
	After contact with the Cr complex solution	3.37
	After contact with only 3-MPN	3.57
O	Before contact with electrolyte	66.1
	After contact with the Cr complex solution	66.1
	After contact with only 3-MPN	66.1

In order to further understand the reasons behind the variations of the TE properties observed, impedance spectroscopy measurements were performed under a 5 K temperature difference, which is a possible temperature gradient for the system under operation using body heat. Fig. S5† shows the impedance spectra for the systems in contact with the Cr complex solution and only the 3MPN. It can be observed that all the impedance spectra show points lying around a specific value of the Z' axis, which indicates the presence of only an ohmic resistance in the system,[10] attributed to the ohmic electronic conduction through the $Sb:SnO_2$ film. The presence of semicircles or other features is not found in any of the spectra after adding the electrolyte, which corroborates that no charge transfer to the electrolyte occurs under operation (no electrical conduction through the liquid), and the only existing process is the ohmic electrical conduction through the film. The impedance spectra were fitted to the equivalent circuit shown in the inset of Fig. S5a† (a resistor) and the fitted parameters with their relative error are included in Table 3. It can be observed that the obtained resistances match with the resistances of Table 1 measured by the I–V curves, as expected.

The variation of the electrical conductivity of the oxide film in the presence of both electrolytes can be explained by the injection of electrons from the electrolyte to the film, since the mobility of the electrons is not expected to change as the films' morphology and composition do not significantly vary as mentioned before. For the case of the systems with only 3-MPN, which is a solvent and is not expected to exchange electrons with the film, a possible mechanism leading to an increase in the number of free electrons can come from the accumulation of electrons at the film/solvent interface after equilibration, which can produce a 'donor effect', since the 3-MPN is a polar molecule. This possible mechanism can be seen in Fig. 10 of ref. 11, and it is observed in SnO_2 when it is used as a humidity sensor.

In the systems with $Cr(acac)_3$, the injection of electrons can be produced by the presence of both the 3-MPN solvent and the $Cr(acac)_3$ complex, which is an electroactive (redox) molecule, employed due to this property in redox flow batteries.[12,13] A higher injection of electrons is expected in the system with the complex, thus leading to a higher reduction of the resistance. It is well known that a reduction in the electrical resistivity of a semiconductor typically produces a decrease in the absolute

Table 3 Resistance values without and with electrolytes extracted from the impedance spectra of Fig. S5. Relative errors from the fitting are indicated in brackets

	Resistance (kΩ)	
	Without electrolyte	With electrolyte
1-Cr	10.9 (0.68%)	2.02 (0.42%)
2-Cr	11.6 (1.00%)	2.16 (0.42%)
3-Cr	11.2 (0.41%)	2.46 (0.39%)
1-3MPN	7.25 (0.82%)	4.28 (0.51%)
2-3MPN	9.77 (0.85%)	6.16 (0.50%)
3-3MPN	8.22 (0.76%)	5.02 (0.79%)

value of the Seebeck coefficient,[6] as observed in Table 1. In this case, a more drastic reduction in the systems with the Cr complex is not clearly observed, as could be expected due to their higher resistance variation. In any case, it should be noted that the differences in the variations produced are not extremely different.

Conclusions

We have studied the possibility of obtaining power factor improvements in a hybrid solid–liquid thermoelectric system. Unlike the electrolytes previously employed, we have used an electrolyte containing an electroactive molecule (chromium acetylacetonate) dissolved in 3-methoxypropionitrile solvent. The electrolyte permeated a nanostructured and porous Sb-doped SnO_2 film. An average power factor improvement of 3.4 times was achieved due to the presence of the electrolyte. The enhancement originated from an average decrease of 23.2% and 82.8% in the absolute value of the Seebeck coefficient and the electrical resistivity of the solid, respectively. Morphological changes and variations in the chemical composition of the films were not observed by SEM and EDX analysis. An impedance spectroscopy study concluded that the power factor improvements are related to the donation of electrons from the electrolyte to the solid, which increases its electrical conductivity and the consequent drop in the Seebeck coefficient. These results show that the hybrid solid–liquid system concept could also be extended to electrolytes with electroactive species, able to exchange electrons with the solid, opening the possibility to study a huge number of possible redox molecules. In addition, it also offers the opportunity to test this new system using nanostructured and porous solids with better thermoelectric performance than Sb:SnO_2, such as Bi_2Te_3, which could lead to extraordinarily high power factors and also overall performance, since the thermal conductivity of the system is not expected to significantly increase due to the porosity of the solid and the low thermal conductivity of liquids (similar to that of polymers). This possibility will be investigated in future work.

Conflicts of interest

There are no conflicts to declare.

Acknowledgements

This project has received funding from the European Union's Horizon 2020 research and innovation programme under grant agreement no. 863222 (UncorrelaTEd project). We also acknowledge funding support from PID2021-122900NB-I00 financed by MICIN/AEI/10.13039/501100011033/FEDER "Una manera de hacer Europa". G. G.-B gratefully acknowledges (RYC2019-026693-I/AEI/10.13039/501100011033) "El Fondo Social Europeo invierte en tu futuro' and Gobierno de Aragón/FEDER, UE (GA/FEDER, Reactividad y catálisis en química inorgánica, Group E50_20D). Raquel Oliver and Pepe Ortega are acknowledged for their technical support.

References

1 J. He and T. M. Tritt, *Science*, 1979, **357**, eaak9997.
2 D. Beretta, N. Neophytou, J. M. Hodges, M. G. Kanatzidis, D. Narducci, M. Martin-Gonzalez, M. Beekman, B. Balke, G. Cerretti, W. Tremel, A. Zevalkink, A. I. Hofmann, C. Müller, B. Dörling, M. Campoy-Quiles and M. Caironi, *Mater. Sci. Eng., R*, 2019, **138**, 210–255.
3 D. Champier, *Energy Convers. Manage.*, 2017, **140**, 167–181.
4 A. R. M. Siddique, S. Mahmud and B. van Heyst, *Renewable Sustainable Energy Rev.*, 2017, **73**, 730–744.
5 Q. Yan and M. G. Kanatzidis, *Nat. Mater.*, 2021, **21**, 503–513.
6 A. Mehdizadeh Dehkordi, M. Zebarjadi, J. He and T. M. Tritt, *Mater. Sci. Eng., R*, 2015, **97**, 1–22.
7 S. Mardi, P. Cataldi, A. Athanassiou and A. Reale, *Appl. Phys. Lett.*, 2022, **120**, 033102.
8 M. Tonga, L. Wei, E. Wilusz, L. Korugic-Karasz, F. E. Karasz and P. M. Lahti, *Synth. Met.*, 2018, **239**, 51–58.
9 L. Márquez-García, B. Beltrán-Pitarch, D. Powell, G. Min and J. García-Cañadas, *ACS Appl. Energy Mater.*, 2018, **1**, 254–259.
10 J. Bisquert and F. Fabregat-Santiago, in *Dye-sensitized Solar Cells*, ed. K. Kalyanasundaram, EPFL Press, 2010, p. 457.
11 Z. Chen and C. Lu, *Sens. Lett.*, 2005, **3**(4), 274–295.
12 M. O. Bamgbopa, Y. Shao-Horn and S. Almheiri, *J. Mater. Chem. A*, 2017, **5**, 13457–13468.
13 Q. Liu, A. A. Shinkle, Y. Li, C. W. Monroe, L. T. Thompson and A. E. S. Sleightholme, *Electrochem. Commun.*, 2010, **12**, 1634–1637.